Supporting information

Schilmiller et al. 10.1073/pnas.1207906109

SI Materials and Methods

PCR Primer List. Virus-induced gene silencing (VIGS) primers containing ligation independent cloning (LIC) cloning adapters:

AT1-F: 5′CGACGACAAGACCCTCATTTTGGGTCAGCCCCGTTG-3′
AT1-R: 5′GAGGAGAAGAGCCCTATTTCCCTTCCTTGATGTTGTGTTATTG-3′
AT2-F: 5′CGACGACAAGACCCTGCCAAGAAAATGCAACAGGTA-3′
AT2-R: 5′GAGGAGAAGAGCCCTATGATCATATGATGAAGTGCTGTTC-3′
AT3-F: 5′CGACGACAAGACCCTACGTTGTCGTCGATGCCTCAAGA-3′
AT3-R: 5′GAGGAGAAGAGCCCTTAGTGGTGCCATAAAAGTCCATC-3′
AT*-F: 5′CGACGACAAGACCCTGTTATTATAGTATCTGTCATCAACCAAATCT-3′
AT*-R: 5′GAGGAGAAGAGCCCTGTGTTAGTGTGCGCCCATTCATT-3′

Primers for creating tomato transformation constructs:

AT2F1-attB: 5′-AAAAAGCAGGCTGCCAAGAAAATGCAACAGGTA-3′
AT2R1-attB: 5′-AGAAAGCTGGGTATGATCATATGATGAAGTGCTGTTC-3′
attB1 adapter: 5′-GGGGACAAGTTTGTACAAAAAAGCAGGCT-3′
attB2 adapter: 5′-GGGGACCACTTTGTACAAGAAAGCTGGGT-3′
pAT2-F1: 5′-CTGCAGTTACACCAAATCAATACATACATACCA-3′
AT2seqR1: 5′-ACGTTGGTTTGTGATGAATGAAGAA-3′
pAT2-R: 5′-CTGCAGTTGGATGAATAAAGTGTTGTTTCTG-3′

Primers for RT-PCR:

AT2-RTf: 5′-GATGAGGCAAGAAGAAAGGATGAT-3′
AT2-RTr: 5′-GTGATGAATGAAGAAGCAACAAGCAA-3′

Acyl Sugar Substrate Preparation. Acyl sugars were collected from IL1-3 plants by washing leaflets (1.5 g dry weight) in 30 mL of extraction solvent [acetonitrile/isopropanol/water 3:3:2 (vol/vol/vol) containing 0.1% (vol/vol) formic acid]. To partially purify acyl sugars, the extract was diluted (1:4) with water, then 20 mL were loaded onto two strong cation exchange solid phase extraction columns (Supleco, 500 mg bed weight) preequilibrated with 10% (vol/vol) acetonitrile. Acyl sugars were collected by eluting from each column with 3 mL 100% acetonitrile. After evaporation to dryness under vacuum, the resulting residue was dissolved in 600 μL 50% (vol/vol) ethanol and used directly in the SlAT2 enzyme assays.

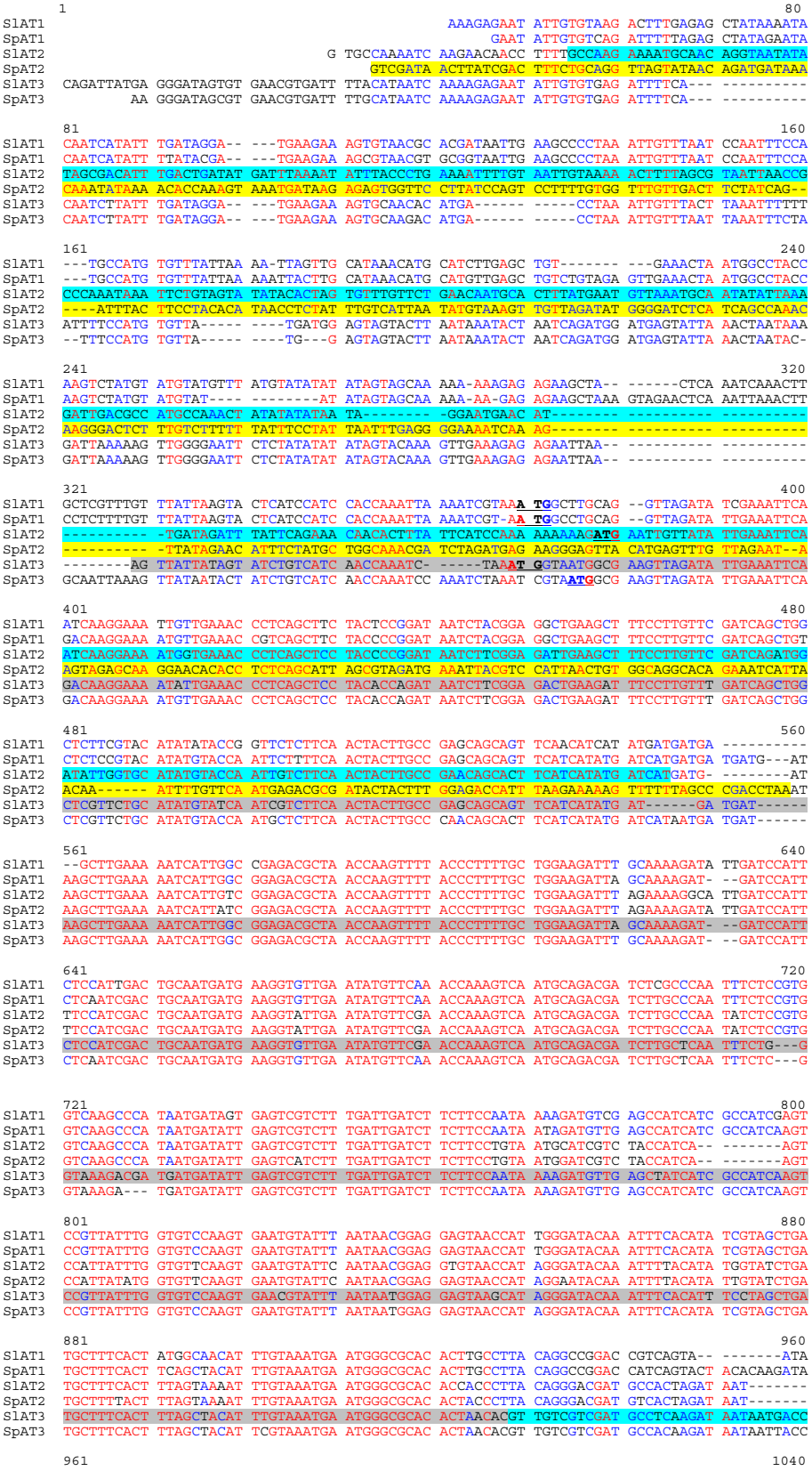

Fig. S1. (Continued)

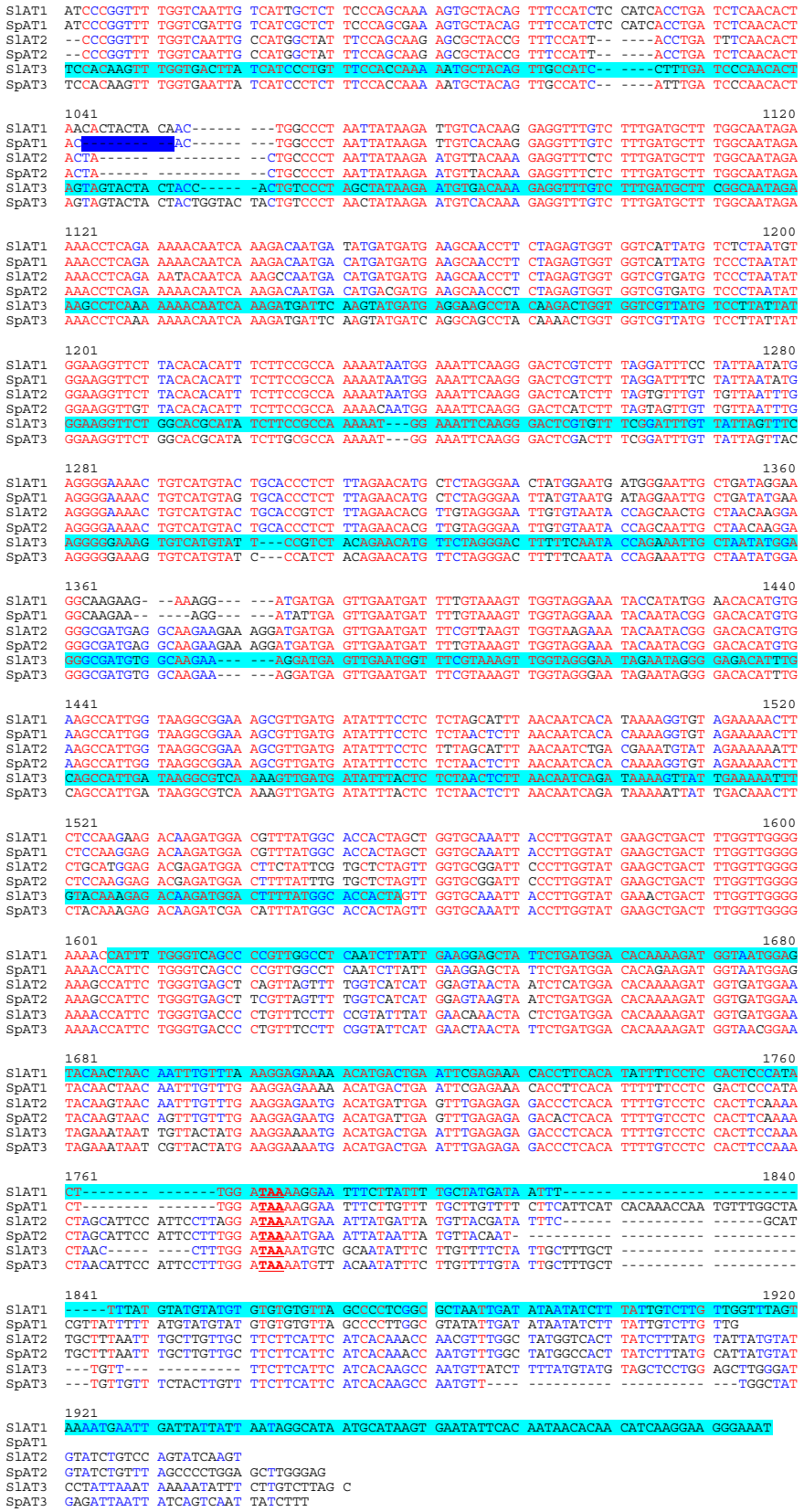

Fig. S1. Sequence alignment of *Solanum lycopersicum* and *Solanum pennellii* chromosome 1 acyltransferase alleles. The region of *SpAT1* containing a 10-bp deletion is highlighted in blue. The 5′ region of *SpAT2* lacking similarity to *SlAT2* is highlighted in yellow. The regions used for creating the VIGS constructs to suppress a single AT gene are highlighted in light blue, and the sequence used to suppress all three AT genes at once is highlighted in gray. Nucleotides where 80% of the sequences match the consensus are red, and those where 50% match the consensus are blue. Start and stop codons are underlined. There are no introns in these genes.

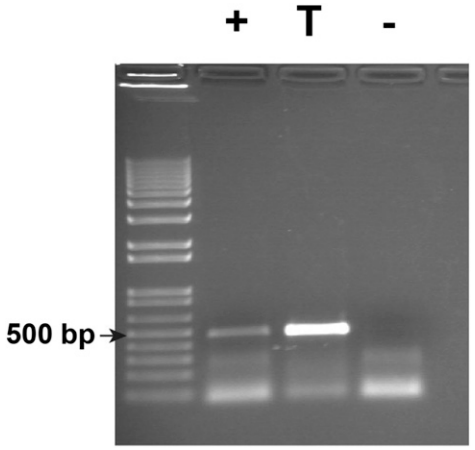

Fig. S2. RT-PCR analysis of *SlAT2* expression. RNA from stem and petiole tissue (+), trichomes isolated from stems and petioles (T), or stem and petiole tissue after removal of trichomes (–) was used for RT-PCR analysis of *SlAT2* expression. Expression was detected in the intact stem and petiole sample, as well as the isolated trichome sample. No *SlAT2* expression was detected in stem and petiole tissue after removal of the trichomes, indicating that expression was primarily in the trichomes.

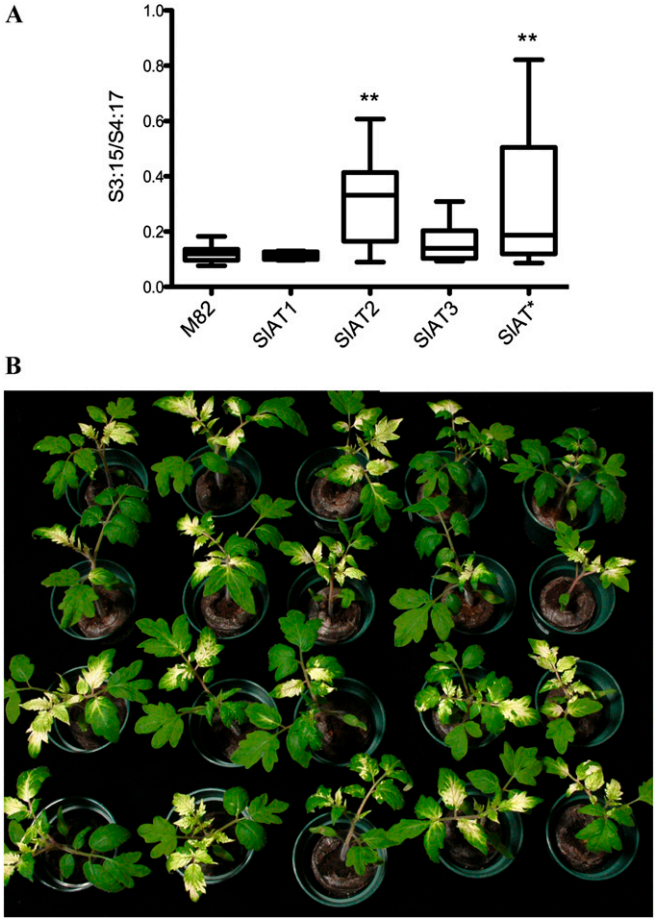

Fig. S3. (*A*) VIGS of *SlAT2* results in an increase in the ratio of unacetylated S3:15 to acetylated S4:17. Sequences for VIGS were chosen either to target a specific *SlAT* mRNA (*SlAT1*, *-2*, and *-3*) or to silence all three genes (*SlAT**). Data are shown as box and whisker plots of the ratios of triacyl sucrose (S3:15) to tetra-acyl sucrose (S4:17), with whiskers showing the minimum and maximum. Only the *SlAT2* and *SlAT** constructs showed a significant change in the ratio of S3:15/S4:17 compared with M82 ($P < 0.05$, Mann-Whitney rank sum test). Similar results were obtained for the ratio of the other pair of major acyl sucroses, S3:22 and S3:24. Sample number: M82 $n = 20$; SlAT1, SlAT2, and SlAT3 $n = 10$; SlAT* $n = 17$. (*B*) Suppression of *phytoene desaturase* (*PDS*) by VIGS in M82 plants illustrating heterogeneous reduction in gene expression.

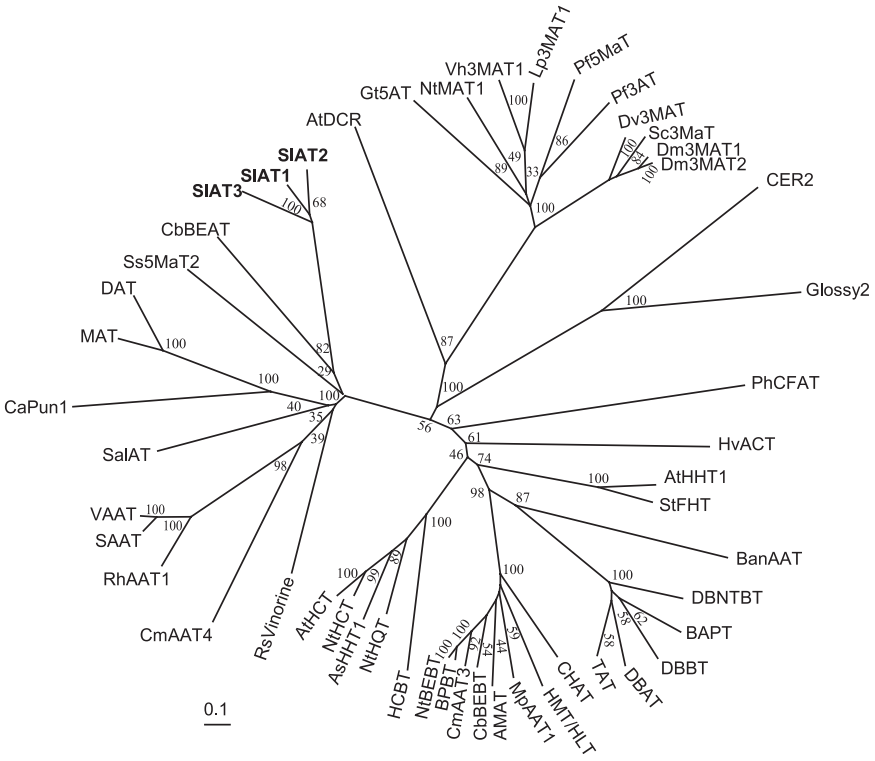

Fig. S4. Phylogeny of a subset of characterized BAHD proteins and SlAT1, -2, and -3. Protein sequences were aligned using MUSCLE (www.ebi.ac.uk/Tools/msa/muscle). An unrooted neighbor-joining phylogeny was inferred using Phylip (http://evolution.genetics.washington.edu/phylip.html). The numbers near the branch points are bootstrap values based on 1,000 replications. GenBank accession numbers: *Zea mays* Glossy2, CAA61258; *Arabidopsis thaliana* CER2, AAM64817; *Petunia x hybrida* PhCFAT, ABG75942; *Hordeum vulgare,* HvACT, AAO73071; *Arabidopsis thaliana*, AtHHT1, AED94629; *Solanum tuberosum* StFHT, FJ825138; *Musa sp*. BanAAT, CAC09063; *Taxus Canadensis* DBNTBT, AAM75818; *Taxus cuspidata* BAPT, AAL92459; *Taxus cuspidate* DBBT, Q9FPW3; *Taxus cuspidata* DBAT, AAF27621; *Taxus cuspidata* TAT, AAF34254; *Arabidopsis thaliana* CHAT, AAN09797; *Lupinus albus* HMT/HLT, BAD89275; *Malus x domestica* MpAAT1, AAU14879; *Vitis labrusca* AMAT, AAW22989; *Clarkia breweri* CbBEBT, AAN09796; *Cucumis melo*. CmAAT3, AAW51125; *Petunia x hybrida* BPBT, AAU06226; *Nicotiana tabacum* NtBEBT, AAN09798; *Dianthus caryophyllus* HCBT, CAB06430; *Nicotiana tabacum* NtHQT, CAE46932; *Avena sativa* AsHHT1, BAC78633; *Nicotiana tabacum* NtHCT, CAD47830; *Arabidopsis thaliana* AtHCT, NP_199704; *Rauvolfia serpentina* RsVinorine, CAD89104; *Cucumis melo* CmAAT4, AAW51126; *Rosa hybrid cultivar* RhAAT1, AAW31948; *Fragaria x ananassa* SAAT, AAG13130; *Fragaria vesca* VAAT, CAC09062; *Papaver somniferum* SalAT, AAK73661; *Capsicum annuum* CaPun1, AAV66311; *Catharanthus roseus* MAT, AAO13736; *Catharanthus roseus* DAT, AAC99311; *Salvia splendens* Ss5MaT2, AAL50566; *Clarkia breweri* CbBEAT, AAC18062; *Solanum lycopersicum,* **SlAT1**, JQ899257; *Solanum lycopersicum,* **SlAT2**, JQ899258; *Solanum lycopersicum,* **SlAT3**, JQ899259; *Arabidopsis thaliana* AtDCR, NP_197782; *Gentiana triflora* Gt5AT, BAA74428; *Nicotiana tabacum* NtMAT1, BAD93691; *Glandularia x hybrida* Vh3MAT1, AAS77402; *Lamium purpureum* Lp3MAT1, AAS77404; *Perilla frutescens* Pf5MaT, AAL50565; *Perilla frutescens* Pf3AT, BAA93475; *Dahlia pinnata* Dv3MAT, AAO12206; *Pericallis cruenta* Sc3MaT, AAO38058; *Chrysanthemum x morifolium* Dm3MAT1, AAQ63615; *Chrysanthemum x morifolium* Dm3MAT2, AAQ63616.

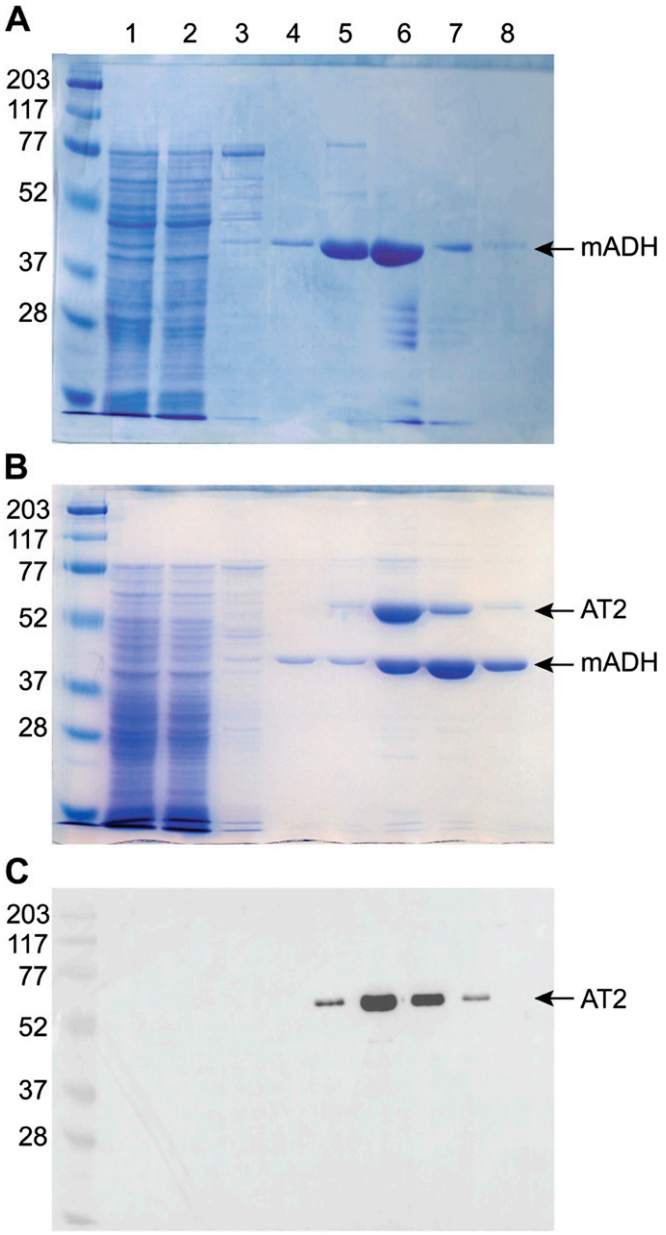

Fig. S5. Purification of recombinant SlAT2 fusion protein from *Pichia pastoris* yeast cells. Total soluble protein isolated from untransformed *Pichia* X33 cells or cells expressing SlAT2 were used for Ni-affinity chromatography. Shown are Coomassie blue-stained SDS/PAGE gels for X33 control (*A*) and SlAT2-expressing cells (*B*). The predicted molecular mass of recombinant SlAT2 is 56 kDa. The other protein binding to the Ni-resin at ~40 kDa was identified by mass spectrometry to be a *Pichia* mitochondrial alcohol dehydrogenase (mADH; GenBank accession CAY69102). (*C*) Results from an immunoblot of a gel identical to *B* that was probed with anti-cMyc-HRP antibody. Lanes are as follows: 1, crude extract; 2, protein not bound to Ni-resin; 3, 20 mM imidazole wash; 4–8, 200-mM imidazole elution fractions. Sizes of protein markers (kDa) are shown on left.

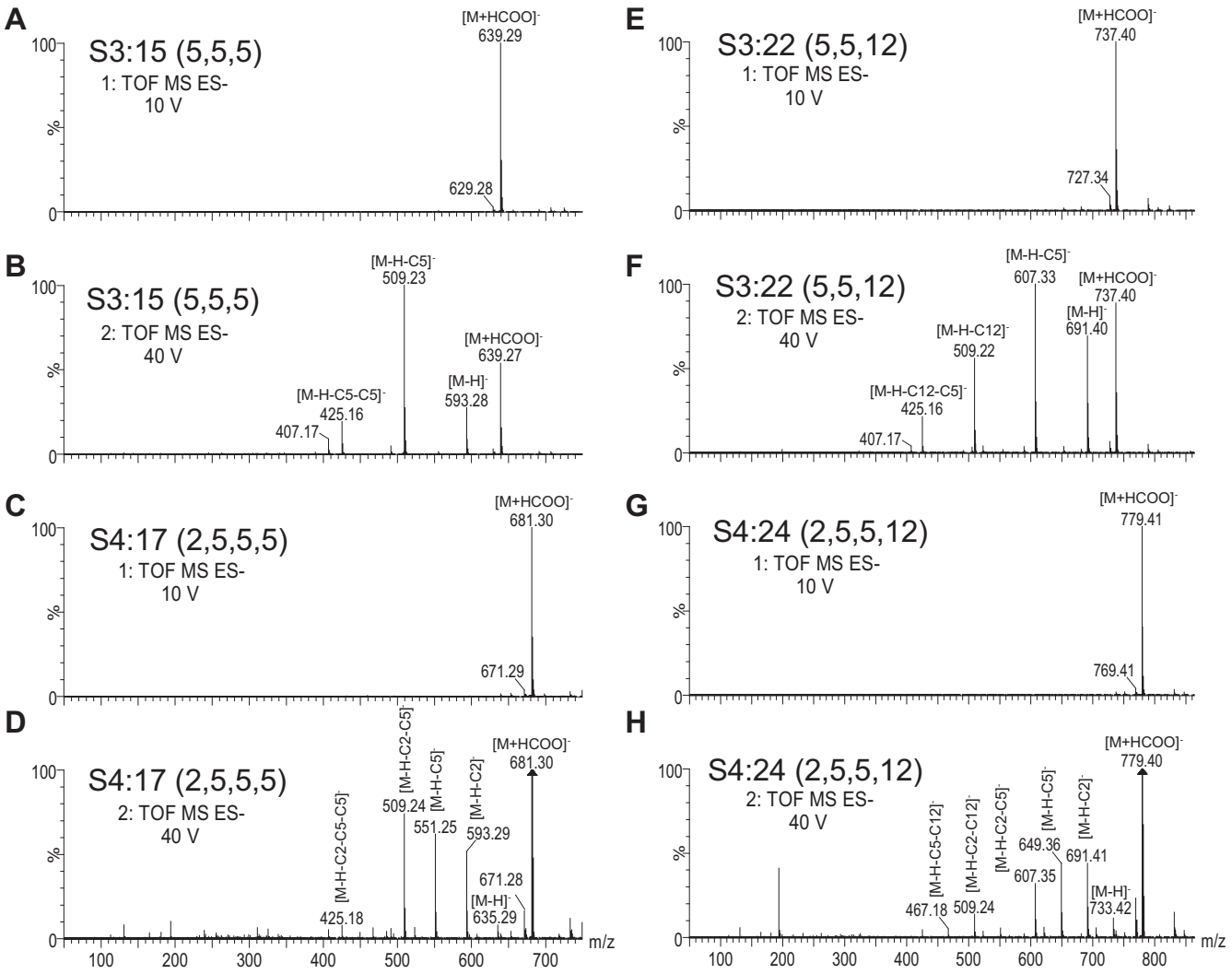

Fig. S6. Negative ion mass spectra of peaks labeled in Fig. 3. Mass spectra of acyl sucroses at low collision energy (10 V; *A*, *C*, *E*, and *G*) show primarily the formate adduct ion. Increasing the collision energy to 40 V (*B*, *D*, *F*, and *H*) results in fragmentation of the acyl sucroses due to loss of acyl chains. For example, the mass spectrum of triacyl sugar substrate S3:15 (5,5,5) at low energy (10 V) shows a formic acid adduct ion at *m/z* 639.29 (*A*). Fragmentation of S3:15 (5,5,5) due to increased energy (40 V) shows appearance of the pseudomolecular ion $(M-H)^-$ at *m/z* 593.28, as well as fragment ions from successive neutral loss of the acyl chains as ketenes of mass 84 Da (*B*). Acetylated acyl sugars show a characteristic $[M-H-C2]^-$ ion that is 42 Da less than the pseudomolecular ion $[M-H]^-$ (for example, *m/z* 593.29 in *D*, and *m/z* 691.41 in *H*).

Table S1. Peak areas from extracted ion chromatograms of the formate adducts of acyl sugars from IL1-3 incubated with an untransformed X33 control or with SlAT2

Acyl sugar	Nominal *m/z* of $[M+formate]^-$	Retention time (min)	X33 control peak area	AT2 peak area ion counts/minute
S3:15 (5,5,5)	639	3.30	2,177.321	1,300.682
S4:17 (2,5,5,5)	681	3.36	10.348	1,164.307
S3:16 (5,5,6)	653	3.37	87.728	26.277
S4:18 (2,5,5,6)	695	3.42	0.637	34.094
S3:20 (5,5,10)	709	3.60	245.849	54.226
S4:22 (2,5,5,10)	751	3.64	ND	139.034
S3:21 (5,5,11)	723	3.63	489.74	190.61
S4:23 (2,5,5,11)	765	3.68	ND	275.356
S3:22 (5,5,12)	737	3.69	2,071.95	1,180.051
S4:24 (2,5,5,12)	779	3.79	30.595	1,662.847
S3:23 (5,6,12)	751	3.72	240.331	48.45
S4:25 (2,5,6,12)	793	3.79	ND	187.259

Acyl sugars were identified according to their *m/z* and retention time, as well as from mass spectra generated using higher collision energy (1). All triacyl sucroses identified were acetylated regardless of the length of the attached acyl chains, as shown by the increase in peak areas for the corresponding tetra-acyl sucroses containing an acetyl group. ND, not detected.

1. Schilmiller A, et al. (2010) Mass spectrometry screening reveals widespread diversity in trichome specialized metabolites of tomato chromosomal substitution lines. *Plant J* 62:391–403.